NASA Technical Memorandum 105764

Current Status of Liquid Sheet Radiator Research

Donald L. Chubb and Frederick D. Calfo
Lewis Research Center
Cleveland, Ohio

and

Matthew S. McMaster
University of Toledo
Toledo, Ohio

Prepared for the
First International Conference on Aerospace Heat Exchanger Technology
sponsored by the AIAA and ASME
Palo Alto, California, February 15–17, 1993

CURRENT STATUS OF LIQUID SHEET RADIATOR RESEARCH

Donald L. Chubb and Frederick D. Calfo

National Aeronautics and Space Administration Lewis Research Center
Cleveland, Ohio 44135, U.S.A.

Matthew S. McMaster

University of Toledo, Toledo, Ohio 43606, U.S.A.

ABSTRACT

Initial research on the external flow, low mass liquid sheet radiator (LSR), has been concentrated on understanding its fluid mechanics. The surface tension forces acting at the edges of the sheet produce a triangular planform for the radiating surface of width, W, and length, L. It has been experimentally verified that L/W agrees with the theoretical result, $L/W = [We/8]^{1/2}$, where We is the Weber number. Instability can cause holes to form in regions of large curvature such as where the edge cylinders join the sheet of thickness, τ. The W/τ limit that will cause hole formation with subsequent destruction of the sheet has yet to be reached experimentally.

Although experimental measurements of sheet emissivity have not yet been performed because of limited program scope, calculations of the emissivity and sheet lifetime as determined by evaporation losses were made for two silicon based oils; D.C. 705 and Me_2. Emissivities greater than 0.75 are calculated for $\tau \geq 200$ μm for both oils. Lifetimes for Me_2 are much longer than lifetimes for 705. Therefore, Me_2 is the more attractive working fluid for higher temperatures ($T \geq 400$ K).

E-7181

CURRENT STATUS OF LIQUID SHEET RADIATOR RESEARCH

Introduction

The liquid sheet radiator (LSR) is an external flow radiator similar in several ways to other external flow radiators such as the liquid droplet [1-3] (LDR) and liquid belt radiators [4,5]. All of these radiator concepts potentially have lower mass than solid wall radiators such as pumped loop and heat pipe radiators. They are also nearly immune to micrometeoroid penetration. However, the LSR has the added advantage of simplicity. As a result of surface tension forces acting at the edges of the sheet, the sheet flow has a triangular shape (Fig.1) which is desirable as it allows collection of the flow at a single point. To obtain a similar triangular area for the LDR requires very accurate aiming of many (10^5 to 10^6) droplet streams.

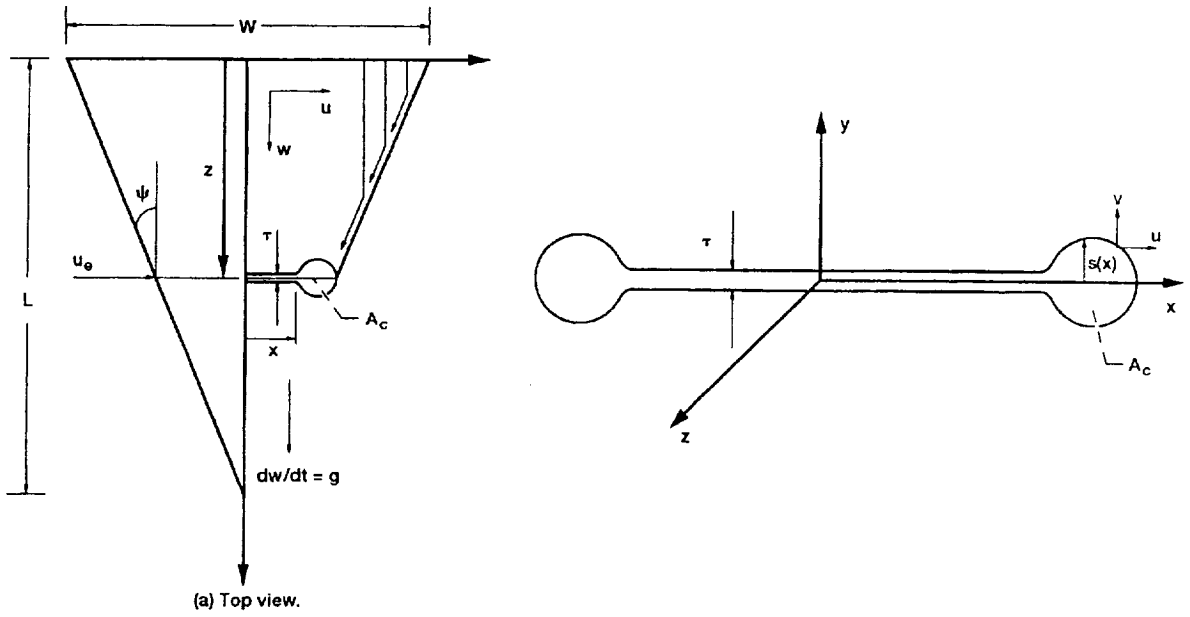

Figure 1.—Schematic of thin liquid sheet flow.

Simplicity of the LSR should also result in lower cost and mass for the LSR compared to the LDR and liquid belt radiators (LBR).

A major problem for all external flow radiators is the requirement that the working fluid have a very low ($<10^{-8}$ Torr) vapor pressure to minimize evaporative losses. As a result, working fluids are limited to certain silicon based oils (such as used in diffusion pumps) for low temperatures (300 to 400 K) and liquid metals for higher temperatures [1].

Figure 1 is a schematic drawing of a liquid sheet flow. Surface tension forces at the two edges of the sheet push the edges toward the z axis. As a result, as the flow moves in the z direction the edge cross-sectioned area, A_c, grows. In order to satisfy mass continuity the edges approach each other and finally meet at the point z = L. Figure 2 is a photograph of a small scale sheet flow of Dow-Corning 704 oil in vacuum. The growth of the edge cylinders can be seen in this photograph. If a gas surrounded the sheet flow the associated drag force would tend to break up the sheet flow. Whether or not sheet breakup occurs depends on the velocity and ratio of the sheet liquid density to the surrounding gas density.

Currently the LSR is only at the research stage of development. No system hardware, other than the narrow slits used to form the sheets, has been developed. However, a schematic drawing of a possible LSR space radiator is shown in Fig. 3. This shows four sheet flows connected in parallel. The number of sheets required for an actual application will be determined by the heat load. The system consists of three main components; a slit ejector, a collector, and a pump to produce the necessary flow. In Fig. 3 a heat exchanger is shown between the thermal load and the sheet flows. This heat exchanger is not necessary if the thermal load is compatible with the sheet liquid. The temperature drop that occurs between the ejector and collector is very small so that the LSR behaves like a constant tempertature radiator, similar to a heat pipe radiator.

Initial research on the LSR has been directed at understanding the fluid mechanics of sheet flows [6,7]. There has also been a systems study [8] of the LSR in low power (2 kW) Closed Brayton (CBC) and Free Piston Stirling (FPS) cycles. In that study, with the LSR mass

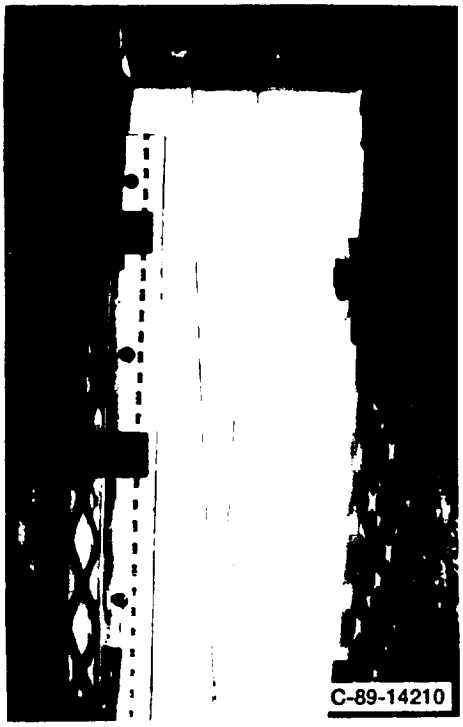

Figure 2.—Sheet flow of Dow-Corning 704 oil in vacuum. Slit thickness = 109 μm, slit width = 3.4 cm, L/W = 9.6.

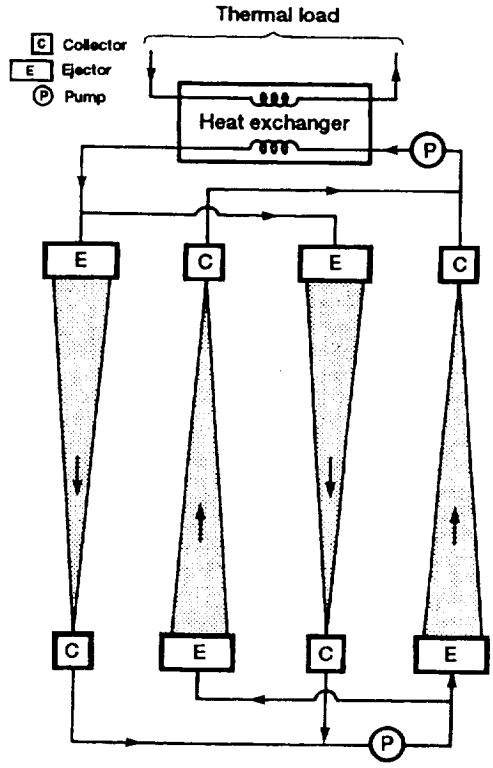

Figure 3.—Schematic of parallel connected liquid sheet radiator system.

estimated to be 1.5 kg/m^2 the LSR was shown to be quite compatible with FPS based space power systems, but not well matched with heat rejection temperature profiles of CBC power systems. However, general conclusions from the study confirmed the applicablility of LSR to space power systems with near constant heat rejection temperatures, including Stirling, Rankine, Thermoelectric, and Thermionic power systems.

This paper presents the latest results for the scaling (L/W = sheet length/sheet width) and the geometry of the edge cylinders. Also, since emissivity and evaporative mass loss are the two most critical properties of a sheet radiator, results of an emissivity calculation and sheet lifetime results based on experimental evaporative loss rates for two possible oils that can be used in the LSR are presented. Finally, mention of LSR research currently in progress and important research yet to be done will be made.

Scaling Results

The surface tension force, dF, at the two edges of the sheet push the edges toward the z axis (Fig. 1). This force is proportional to the surface tension, σ, and inversely proportional to the radius of curvature R_c. As the flow moves in the z direction the edge cross-sectional area, A_c, grows. In order to satisfy mass continuity the edges approach each other and finally meet at the point z = L.

If the surface tension force per unit length, $\frac{dF}{dz}$, is equated to the rate of momentum change per unit length, $\rho\tau u_e^2$, where ρ is the density, τ is the sheet thickness, and u_e is the edge velocity, then relations for u_e and L/W can be obtained [7].

$$u_e = \left(\frac{2\sigma}{\rho\tau}\right)^{1/2} \tag{1}$$

For the case where there is no force (gravity for example) acting in the z direction the sheet thickness τ, is a constant. As a result the edge velocity, u_e, will be constant [7] and;

$$\frac{L}{W} = \left(\frac{We}{8}\right)^{1/2} \tag{2}$$

Where the Weber number, We, is defined as:

$$We = \frac{\rho\tau w_o^2}{\sigma} \tag{3}$$

where w_o is the velocity in the z direction. As can be seen from Eqs. (2) and (3), L/W is a linear function of velocity, w_o.

A large amount of L/W data for D.C. 705 oil has been obtained in a vacuum facility [7] which can accommodate sheet flows with $W \leq 25$ cm and $L \leq 3.5$ m. These results are shown in Fig. 4. Note the good agreement between the theoretical result (Eq. (2)) and the experimental data. For a practical radiator $L/W \approx 10$ so that $We \approx 1000$. The temperature dependence of ρ and σ for Dow-Corning 705 is given by [9]:

$$\rho = 1569 - 1.625\ T\ kg/m^3 \qquad T = K \tag{4}$$

$$\sigma = \left(86.14 - \frac{T}{6.5}\right) \times 10^{-3}\ n/m \qquad T = K \tag{5}$$

All the data in Fig. 4 was taken with $T = 371$ K. For D.C. 705 oil $0.025 < \sigma < 0.040$ n/m for $400 > T > 300$ K, which is the temperature range where the silicone oils have sufficiently low vapor pressure. For higher temperature operation liquid metals [1] are the only fluids with low enough vapor pressure to have minimal evaporative losses for space applications. The surface tension [1], σ, of liquid metals is at least an order of magnitude larger (0.3 to 0.9 n/m) than that for silicone oils. Whereas, the densities of the liquid metals of interest range from one-half (lithium) the density of D.C. 705 to 12 times D.C. 705 density for mercury. Therefore, for a given sheet thickness, τ, the low density metals such as lithium and aluminum require a significantly higher velocity than a silicone oil to obtain the same Weber number. For a silicone oil $w_o \approx 10$ m/sec yields $We \approx 1000$ for $\tau = 200$ μm. However, for a low mass liquid metal such as lithium $w_o \approx 60$ m/sec for $We = 1000$ and $\tau = 200$ μm. The other liquid metals will require velocities of 10 to 60 m/sec to obtain We = 1000 for

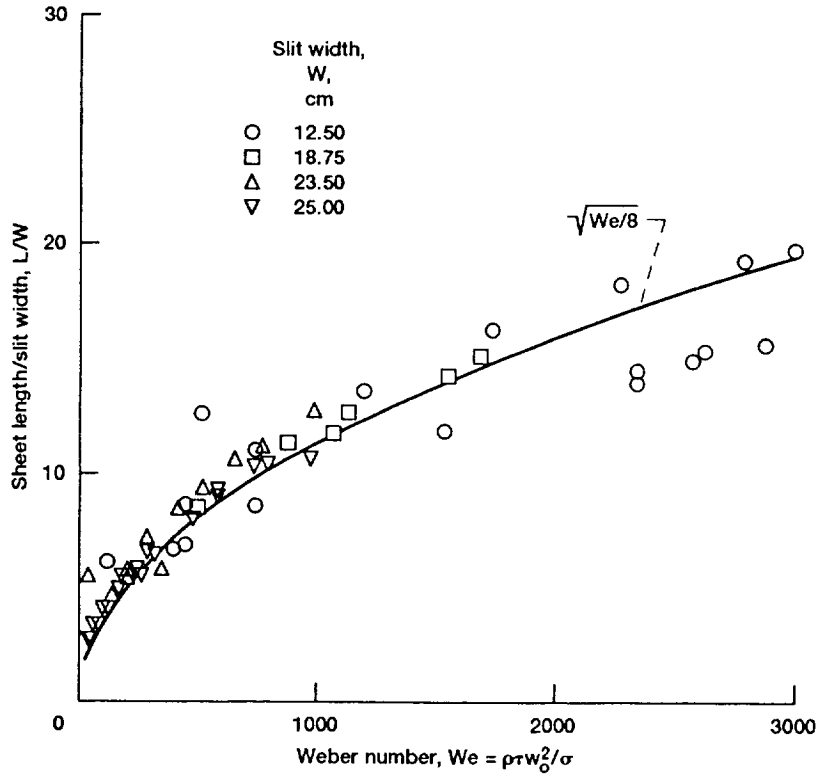

Figure 4.—Comparison of theoretical and experimental sheet scaling.

$\tau = 200$ μm. The higher velocities required by the liquid metals coupled with their higher densities translates to significantly larger pump power than that required for the silicone oils.

Sheet Stability and Edge Cylinder Geometry

Another critical fluid mechanical problem is sheet stability. Linear stability theory for an infinite sheet [11] predicts no instability (i.e., no solutions that grow in time). However, if the sheet is not planar everywhere, such as occurs at the sheet edge cylinders, then linear theory does predict growing solutions in the nonplanar regions. These results were obtained in a study that has not yet been completed and hence will be reported elsewhere. However, some highlights and general observations are discussed below.

Holes have been observed to form where the edge cylinder joins the sheet but are quickly swept downstream before they have a chance to grow significantly. However, as τ decreases the hole growth rate will increase. It is expected that there will be a limit on W/τ to insure that a hole will not form and then grow fast enough to eliminate the sheet. Experimentally this W/τ limit has not been reached. However, an experiment is being set up to determine it.

Since instability is expected to occur in the edge cylinder region, a study of the edge cylinder geometry was made. In Fig. 5 a representation of the edge cylinder geometry at four z (flow direction) locations is shown. Experimentally it has been found that the edge cylinder geometry oscillates in the z direction between nearly a circle to a highly elliptical shape then a "peanut" like shape and finally back to nearly a circle as shown in Fig. 5.

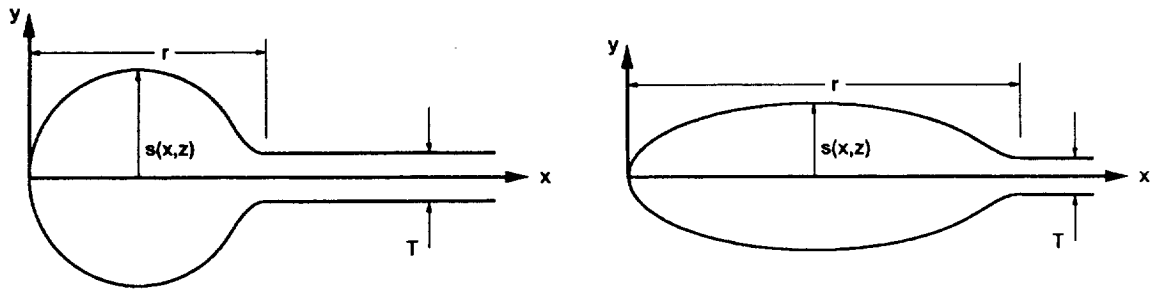

(a) Initial, nearly circular cross-sectional shape.

(b) Flattened out cross-sectional shape.

(c) Rebuilding or peanut like cross-sectional shape.

(d) Larger, rebuilt, nearly circular cross-sectional shape.

Figure 5.—Schematic of edge cylinder variation in flow direction.

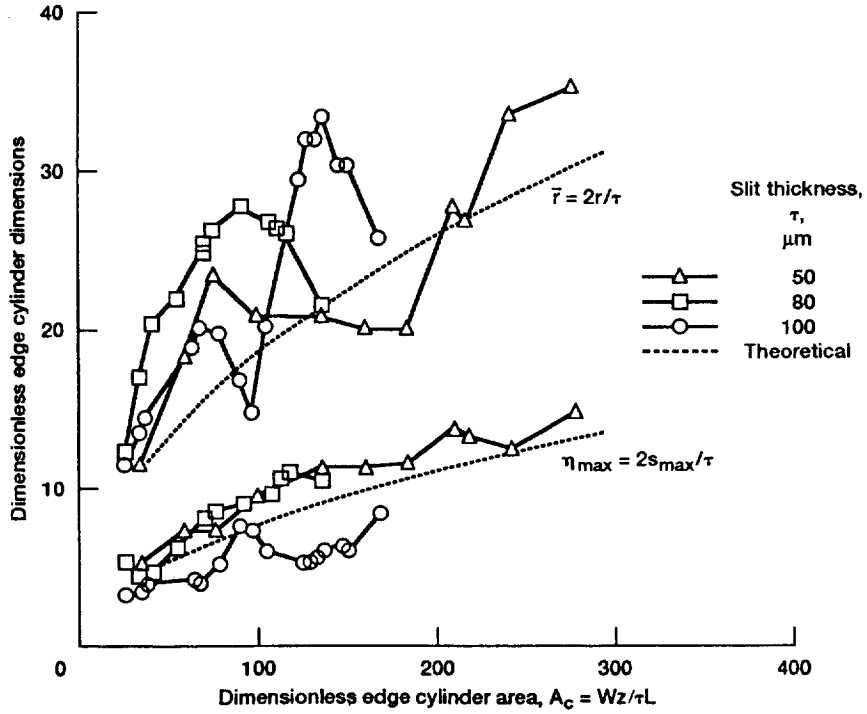

Figure 6.—Comparison of experimental and theoretical edge cross section dimensions.

The theoretical analysis predicts a nearly circular geometry for the edge cylinder. No highly elliptical or peanut like solutions were found. In Fig. 6 a comparison between the experimental and theoretical edge cylinder geometry results is made. Experimental results for three sheet thicknesses, $\tau = 50$, 80, and 100 μm are shown. The dimensionless width of the edge cylinder, $\bar{r} = 2r/\tau$, and dimensionless maximum height of the edge cylinder, $\eta_{MAX} = 2s/\tau$, are plotted as a function of the dimensionless edge cylinder cross sectional area, $\bar{A}_c = 2A_c/\tau^2 = Wz/\tau L$ (from mass continuity and the fact that the sheet is triangular it can be shown that the edge cylinder area is a linear function of z). The results for the $\tau = 100$ μm sheet agree well with the model shown in Fig. 5. For small $\bar{A}_c$ the experimental $\bar{r}$ and η_{MAX} values are close to the nearly circular theoretical results. (For a perfect circle $\bar{r} = 2\ \eta_{MAX}$.) However, as $\bar{A}_c$ increases, $\bar{r}$ increases while η_{MAX} decreases below the theoretical result, indicating the highly elliptical shape is being formed. Then at $\bar{A}_c \approx 75$, $\bar{r}$ starts to decrease toward the theoretical result as η_{MAX} increases toward its theoretical result, indicating that a nearly circular shape is again being formed. Then, at $\bar{A}_c \approx 100$ the cycle begins again. Only from photographic results is it known that the peanut like shape occurs. For the $\tau = 50$ and 80 μm cases both $\bar{r}$ and η_{MAX} remain above the theoretical result for all $\bar{A}_c$. For $\tau = 80$ μm a single oscillation from nearly circular geometry to elliptical shape and then back to a circular shape can be seen. Whereas for $\tau = 50$ μm two such oscillations are seen.

All the data in Fig. 6 indicate an elliptical geometry with $\bar{r} > 2\ \eta_{MAX}$. The more flattened the cross section ($\bar{r} >> 2\ \eta_{MAX}$), the smaller the curvature ($1/R_c$) will be at the point where the edge joins the sheet. The instability growth rate is proportional to the curvature. Therefore, the flattened edge cross section regions are less likely than the more circular regions to result in hole formation.

Properties of Possible Silicone Oils for the LSR

Low vapor pressure is a necessity for the working fluid of an external flow radiator. However, for an efficient radiator the working fluid emissivity must also be large. Fortuitously, for the temperature range of interest (300 to 400 K) we find that the silicone oils, which are transparent to visible radiation, do have sufficiently high emissivity for space radiator applications. This emissivity results from a high absorption coefficient in the wavelength region ($8 < \lambda < 15$ μm) where most of the radiation occurs for temperatures of 300 to 400 K. In other words, the silicone oils behave like a black body in the $8 < \lambda < 15$ μm region, as shown in Table 1.

Previously [7] the emissivity of Dow-Corning 705 oil (D.C. 705) was calculated based on measured transmission data. These results are shown in Fig. 7. However, the evaporation rate for 705 oil is higher than desired. Several new organosiloxane oils [10] have been developed that have much lower evaporation rates. The oil with the lowest evaporation rate is designated Me_2 in Ref. 10. To evaluate the effect of the evaporation rate on the mass of a sheet radiator system, consider the lifetime, t_v, of the sheet mass, M_s.

$$M_s = \rho\tau A_{RAD} = \dot{m}_v t_v A_{RAD} \tag{6}$$

TABLE 1.—ABSORPTION COEFFICIENT FOR DOW—CORNING Me_2 OIL

Wavelength range, μm	Absorption coefficient, a, μm^{-1}
0 to 2.5	0
2.5 to 7.0	8.0×10^{-4}
7.0 to 7.7	6.4×10^{-3}
7.7 to 8.0	1.75×10^{-2}
8.0 to 8.7	1.10×10^{-2}
8.7 to 10.5	1.75×10^{-2}
10.5 to 11.1	1.10×10^{-2}
11.1 to 15.4	1.75×10^{-2}
15.4 to 20.0	6.4×10^{-3}
20.0 to 23.5	5.7×10^{-3}
23.5 to 40	1.07×10^{-2}
40 to 100	1.25×10^{-3}
100 to ∞	0

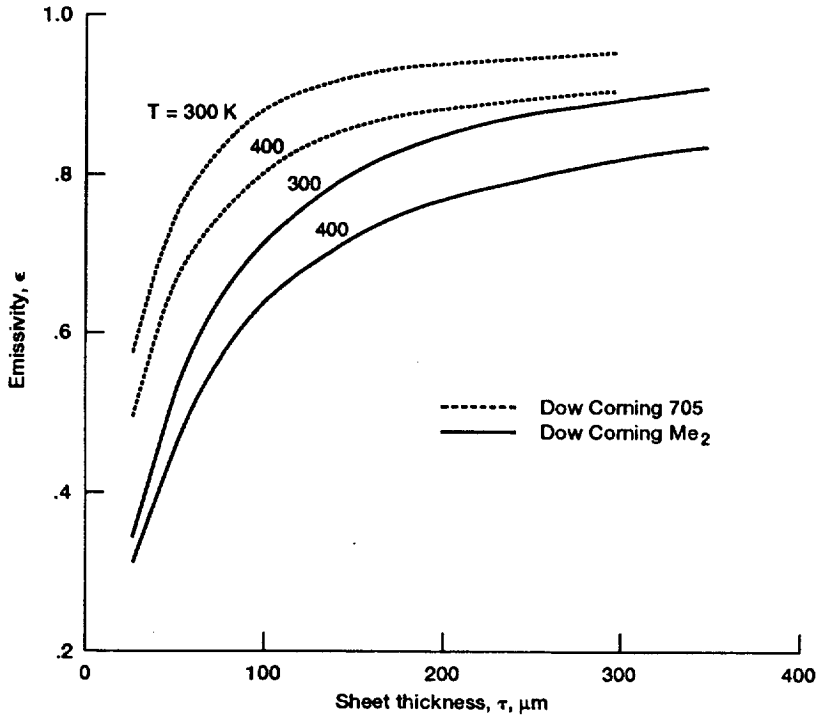

Figure 7.—Calculated emissivity of Dow Corning silicone oils for temperatures of 300 and 400 K.

Therefore,

$$t_v = \frac{\rho\tau}{\dot{m}_v} \tag{7}$$

where $\dot{m}_v$ is the evaporation rate in kg/m^2 sec and A_{RAD} is the total radiating area. If t_L is the desired lifetime of the sheet radiator then the required extra fluid mass, M_{ST}, that must be available to make up for evaporation loss is the following.

$$M_{ST} = M_s\left(\frac{t_L}{t_v}\right) \tag{8}$$

Using the experimental results for D.C. 705 and Me_2 [9,10], t_v was calculated as a function of temperature, T. For D.C. 705 the mass loss rate, m_v, was calculated using the experimental vapor pressure which was curve fit with the following expression [9].

$$\log_{10}p_v = 12.31 - \frac{6490}{T} \qquad T = K,\ p_v = Torr \tag{9}$$

Assuming the evaporation rate is given by Knudsen effusion, then

$$\dot{m}_v = \frac{1}{4}\rho\left(\frac{8kT}{\pi m}\right)^{1/2} = p_v\left(\frac{m}{2\pi kT}\right)^{1/2} \tag{10}$$

where m is the mass of an oil molecule (atomic weight, of D.C. 705 = 546). Equations (4) and (10) were used to calculate t_v for D.C. 705. However, experimental results [10] for m_v that are curve fit with the following expression were used for Me_2.

$$\log_{10}\dot{m}_v = 13.82 - \frac{10197}{T} \qquad T = K,\ \dot{m}_v = Kg/m^2\ sec \tag{11}$$

Also, experimental results [10] for ρ are curve fit with the following result

$$\rho = 1221 - 0.8878\ T \qquad Kg/m^3 \tag{12}$$

and are used to calculate t_v for Me_2. It should be noted that $\dot{m}_v$ calculated using Eq. (10) for Dow-Corning 704 oil in Ref. 10 is an order of magnitude greater than the experimental values for $\dot{m}_v$. If this same result holds true for D.C. 705 then the calculated values of $\dot{m}_v$ using Eq. (10) may be an overestimate. As a result, the calculated lifetimes, t_v, for D.C. 705 may be greatly underestimated.

Results of the t_v calculations are shown in Fig. 8 for τ = 100, 200, and 300 μm. For Me_2 the evaporative loss is so low that $t_v > 10$ yr for $T < 440$ K. Thus, the required extra fluid, $M_{ST} < M_s$ for $t_L < 10$ yr for $T \approx 440$K. For $T \leq 400$ K, $M_{ST} < 0.01\ M_s$ for $t_L = 10$ yr. In this case ($T < 400$ K) negligible extra fluid mass is required. For D.C. 705 oil the evaporation rate is much higher. As a result, for $t_L = 10$ yr the temperature, $T < 300$ in order for $M_{st} < 0.1M_s$.

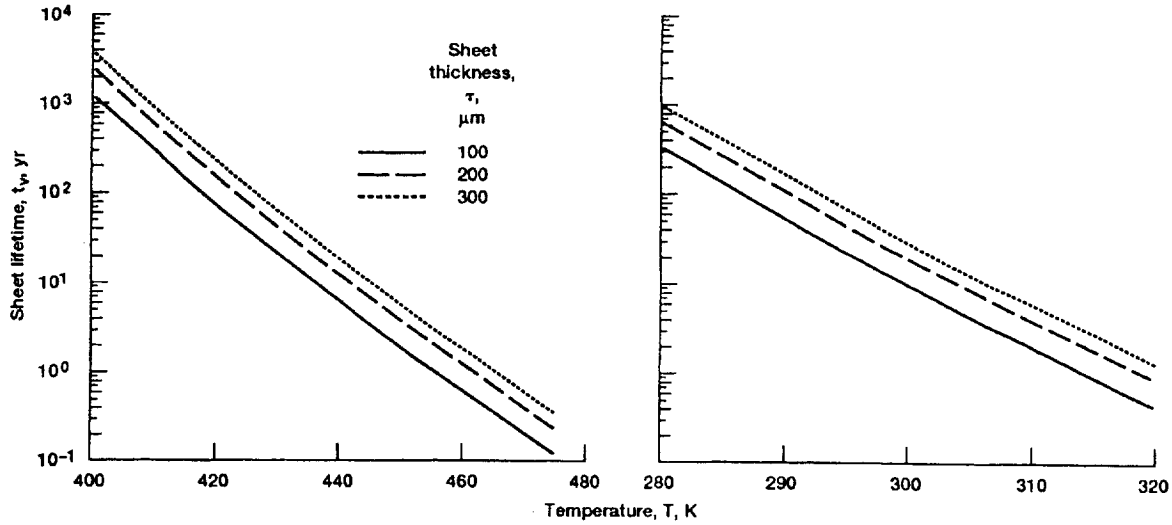

(a) Sheet lifetime for Dow Corning Me_2 oil.

(b) Sheet lifetime for Dow Corning 705 oil.

Figure 8.—Sheet lifetimes for Dow Corning silicone oils Me_2 and 705.

From these results we would conclude that Me_2 will make a better working fluid than D.C. 705. However, the emissivity must also be considered.

To calculate the emissivity of Me_2 the experimental spectral transmission data [10] for 100 and 200 μm films was used. This calculation is similar to the one for D.C. 705 [7]. The experimental spectral transmission data is divided into wavelength bands of constant transmittance. From the experimental transmittance the absorption coefficient for each of the wavelength bands is calculated using the spectral transmittance relation for an infinite sheet [6,7,12].

$$T_\lambda = 2E_3(a_\lambda \tau) \tag{13}$$

where a_λ is the absorption coefficient and $E_3(x)$ is the exponential integral.

$$E_3(x) = \int_0^1 u e^{-x/u}\, du \tag{14}$$

Knowing a_λ the emissivity, ε, can then be calculated [12].

$$\varepsilon = \int_0^\infty \varepsilon_\lambda e_{\lambda b} \frac{d\lambda}{\sigma_{SB} T^4} \tag{15}$$

where σ_{SB} is the Stefan-Boltzmann constant (5.67×10^{-8} W/m^2 K^4) and $e_{\lambda b}$ is the black body hemispherical spectral emissive power [12] and the spectral emittance is the following [12].

$$\varepsilon_\lambda = 1 - T_\lambda = 1 - 2E_3(a_\lambda \tau) \tag{16}$$

For the temperature range of interest (300 to 400 K), $e_{\lambda b} \rightarrow 0$ for $\lambda \leq 4$ μm and $\lambda \geq 70$ μm. Therefore, to calculate ε, it is necessary to know a_λ in the spectral region $4 \leq \lambda \leq 70$ μm. The experimental transmission data of Ref. 10 was split into 13 wavelength bands and the absorption coefficient for each of these bands was determined as described above. These results are shown in Table 1. Using this data the integral in Eq. (11) is split into 13 wavelength bands with ε_λ constant within each band. The emissivity can then be calculated using the tabulated values of

$$F_{\lambda_1 T - \lambda_2 T} = \frac{1}{\sigma_{SB} T^4} \int_{\lambda_1 T}^{\lambda_2 T} e_{\lambda b} d\lambda \tag{17}$$

from Ref. 12. The results of this calculation for Me_2 are compared to the ε results for D.C. 705 in Fig. 7. As can be seen, D.C. 705 has a higher emissivity than Me_2. However, even for Me_2, $\varepsilon > 0.75$ for $\tau > 200$ μm. Thus, the high absorption coefficient in the wavelength region $8 < \lambda < 15$ μm (Table 1) results in acceptable emissivity even though the silicone oils are transparent in the visible wavelength region. For temperatures close to 300 K where evaporation loss for 705 is small, the larger values of ε make D.C. 705 more attractive as a working fluid than Me_2. However, for $T \approx 400$ K the evaporation loss for D.C. 705 is too large and Me_2 is the more desirable working fluid.

RESEARCH IN PROGRESS AND RESEARCH TO BE DONE

Currently research is concentrated in two areas. First, the stability limit of the sheet flow is being experimentally determined. As discussed earlier, there is a limit on W/τ to insure that holes will not form and destroy the sheet. A stability analysis is also being carried out to compare sheet stability predictions with the experimentally measured W/τ limit. The main component of the experimental apparatus is a variable slit with limits of $10\ \mu m < \tau < 100\ \mu m$.

The second area being experimentally investigated is the sheet emissivity. Using the facility described in Ref. 7 the emissivity of D.C. 705 oil will be measured, pending program funding. The emissivity will be determined by measuring the enthalpy, i.e., temperature change of the fluid between the slit and the coalescence point.

Collection of the sheet flow at the coalescence point is the remaining area for research. However, a large amount of collector work [13-15] for the liquid droplet radiator (LDR) may be applicable to the LSR. It may be possible to recover some of the kinetic energy of the sheet flow with a collector that is designed like a subsonic diffuser of a wind tunnel. The collector is the remaining undefined component for an LSR system. Before a prototype LSR can be built, the collector problem must be solved.

CONCLUSION

The fluid mechanics of liquid sheet flows has been extensively researched. Scaling of the flow has been found to satisfy the theoretical result $L/W = [We/8]^{1/2}$. Stability of the flow is currently being investigated. The limit on W/τ is being experimentally determined.

Emissivity, ε, and sheet lifetime, t_v, resulting from evaporation loss have been calculated for two possible LSR working fluids. In the case of D.C. 705 silicone oil, its larger emissivity and acceptable lifetime at $T \approx 300$ K make it attractive for use at the lower temperatures. However, at $T \approx 400$ K the lifetime for D.C. 705 is short (< 1 yr), so that Dow-Corning Me_2, which has $t_v > 10^3$ yr at 400 K, becomes the more desirable fluid.

Currently an experimental measurement of the sheet emissivity is being planned. The remaining research problem that has not been studied is the collection of the sheet flow.

NOMENCLATURE

A_c	Cross-sectional area of edge cylinder, m^2
A_{RAD}	Total radiating area of sheet = WL, m^2
a_λ	Spectral absorption coefficient, m^{-1}
$E_3(x)$	Exponential integral defined by Eq. (14)
e_b	Black body hemispherical spectral emissive power, $w/m^2\ \mu m$
k	Boltzmann constant, 1.38×10^{-23} j/k
L	Length of sheet in flow direction, m
M_s	Mass of sheet fluid, kg
M_{ST}	Required extra fluid mass to make up for evaporation loss, kg
m	Mass of oil molecule of sheet fluid, kg
$\dot{m}_v$	Evaporation rate for sheet fluid, kg/m^2 sec
p_v	Vapor pressure of sheet fluid, n/m^2
R_c	Radius of curvature, m^{-1}
r	Width of edge cylinder in x direction, m
s	Height of edge cylinder in y direction, m
T	Temperature of sheet fluid, K
T_λ	Spectral transmission coefficient of sheet fluid
t_v	Lifetime of sheet fluid, yr
t_L	Desired lifetime of sheet radiator system, yr
u_e	Velocity of sheet edge in x direction, m/sec
W	Width of sheet, m
We	Weber number for sheet flow = $\rho\frac{\tau w_o^2}{\sigma}$
w_o	Sheet flow velocity in z direction
x	Coordinate in plane of sheet and perpendicular to flow direction (z)
y	Coordinate perpendicular to plane of sheet and perpendicular to flow direction (z)
z	Coordinate in plane of sheet and in flow direction
ε	Sheet emissivity
ε_λ	Spectral emittance
η	Dimensionless sheet edge cylinder height = $2s/\tau$
λ	Wavelength, m
ρ	Density of sheet fluid, kg/m^3
σ	Surface tension of sheet fluid, n/m
σ_{SB}	Stefan-Boltzmann constant, 5.67×10^{-8}, $w/m^2\ K^4$
τ	Thickness of sheet, m

REFERENCES

1. Mattick, A.T.; and Hertzberg, A.: Liquid Droplet Radiators for Heat Rejection in Space. J. Ener., vol. 5, no. 6, 1981, pp. 387-393.

2. Mattick, A.T.; and Herzberg, A.: The Liquid Droplet Radiator – An Ultralightweight Heat Rejection System for Efficient Energy Conversion in Space. Acta Astronautic., vol. 9, no. 3, 1982, pp. 165-172.

3. Taussig, R.T.; and Mattick, A.T.: Droplet Radiator Systems for Spacecraft Thermal Control. J. Spacecr. Rockets, vol. 23, no. 1, 1986, pp. 10-17.

4. Teagan, W.P.; and Fitzgerald, K.F.: Preliminary Evaluation of a Liquid Belt Radiator for Space Applications. NASA CR-174807, 1984.

5. Teagan, W. P.; and Fitzgerald, K.F.: Liquid Belt Radiator Design Study. NASA CR–174901, 1986.

6. Chubb, D.L.; and White, K.A., III: Liquid Sheet Radiator. NASA TM-89841, 1987. (Also, AIAA Paper 87-1525, 1987.)

7. Chubb, D.L.; and Calfo, F.D.: Scaling Results for the Liquid Sheet Radiator. Proceedings of the Twenty-Fourth Intersociety Energy Conversion Engineering Conference, W.D. Jackson and D.A. Hull, eds., Vol. 1, IEEE, New York, 1989, pp. 45-50. (Also, NASA TM-102100, 1989.)

8. Juhasz, A.J.; and Chubb, D.L.: Design Considerations for Space Radiators Based on the Liquid Sheet (LSR) Concept. Proceedings of the 26th Intersociety Energy Conversion Engineering Conference, Vol. 6, IEEE, New York, 1991, pp. 48-53.

9. Dow Corning Corp., Midland, Michigan 48640.

10. Buch, R.R.; and Huntress, A.R.: Organosiloxane Working Fluids for the Liquid Droplet Radiator. NASA CR-175033, 1985.

11. Taylor, G.I.: The Dynamics of Thin Sheets of Fluid. II.: Waves on Fluid Sheets. Proc. R. Soc. London, vol. A253, 1959, pp. 296-312.

12. Siegel, R.; and Howell, J.R.: Thermal Radiation Heat Transfer. Second ed. Hemisphere Publishing Corp., Washington, DC, 1981, pp. 19, 52, 612.

13. Mattick, A.T.; and Hertzberg, A.: Advanced Radiator Systems for Space Power. IAF Paper 87-230, 1987.

14. Calia, V., et al.: Liquid Droplet Radiator Collector Development. IECEC-84; 19th Intersociety Energy Conversion Engineering Conference, Vol. 1, IEEE, New York, 1984, pp. 216-223.

15. Konopka, W.; Calia, V.; and Brown, R.: Liquid Droplet Radiation Passive Collector Testing. Proceedings of 20th Intersociety Energy Conversion Engineering Conference, Vol 1, IEEE, New York, 1985, pp. 1.430-1.438.

REPORT DOCUMENTATION PAGE

Form Approved
OMB No. 0704-0188

1. AGENCY USE ONLY (*Leave blank*)	2. REPORT DATE	3. REPORT TYPE AND DATES COVERED
	February 1993	Technical Memorandum

4. TITLE AND SUBTITLE

Current Status of Liquid Sheet Radiator Research

5. FUNDING NUMBERS

WU-506-41-11

6. AUTHOR(S)

Donald L. Chubb, Frederick D. Calfo, and Matthew S. McMaster

7. PERFORMING ORGANIZATION NAME(S) AND ADDRESS(ES)

National Aeronautics and Space Administration
Lewis Research Center
Cleveland, Ohio 44135-3191

8. PERFORMING ORGANIZATION REPORT NUMBER

E-7181

9. SPONSORING/MONITORING AGENCY NAMES(S) AND ADDRESS(ES)

National Aeronautics and Space Administration
Washington, D.C. 20546-0001

10. SPONSORING/MONITORING AGENCY REPORT NUMBER

NASA TM-105764

11. SUPPLEMENTARY NOTES

Prepared for the First International Conference on Aerospace Heat Exchanger Technology sponsored by the AIAA and ASME, Palo Alto, California, February 15-17, 1993. Donald L. Chubb and Frederick D. Calfo, NASA Lewis Research Center, Cleveland, Ohio; and Matthew S. McMaster, University of Toledo, Toledo, Ohio 43606. Responsible person, Donald L. Chubb, (216) 433-2242.

12a. DISTRIBUTION/AVAILABILITY STATEMENT

Unclassified - Unlimited
Subject Categories 20 and 34

12b. DISTRIBUTION CODE

13. ABSTRACT (*Maximum 200 words*)

Initial research on the external flow, low mass liquid sheet radiator (LSR), has been concentrated on understanding its fluid mechanics. The surface tension forces acting at the edges of the sheet produce a triangular planform for the radiating surface of width, W, and length, L. It has been experimentally verified that L/W agrees with the theoretical result, $L/W = [We/8]^{1/2}$, where We is the Weber number. Instability can cause holes to form in regions of large curvature such as where the edge cylinders join the sheet of thickness, τ. The W/τ limit that will cause hole formation with subsequent destruction of the sheet has yet to be reached experimentally. Although experimental measurements of sheet emissivity have not yet been performed because of limited program scope, calculations of the emissivity and sheet lifetime as determined by evaporation losses were made for two silicon based oils; Dow Corning 705 and Me_2. Emissivities greater than 0.75 are calculated for $\tau \geq 200$ μm for both oils. Lifetimes for Me_2 are much longer than lifetimes for 705. Therefore, Me_2 is the more attractive working fluid for higher temperatures ($T \geq 400$ K).

14. SUBJECT TERMS

Liquid sheet; Space radiator; Thin sheet flow; Emissivity of thin sheets

15. NUMBER OF PAGES

14

16. PRICE CODE

A03

17. SECURITY CLASSIFICATION OF REPORT	18. SECURITY CLASSIFICATION OF THIS PAGE	19. SECURITY CLASSIFICATION OF ABSTRACT	20. LIMITATION OF ABSTRACT
Unclassified	Unclassified	Unclassified	